Published for SISSA by Springer

Received: November 8, 2018
Revised: January 17, 2019
Accepted: February 1, 2019
Published: February 15, 2019

Production of $t\bar{t}$ pairs via $\gamma\gamma$ fusion with photon transverse momenta and proton dissociation

Marta Łuszczak,[a] **Laurent Forthomme,**[b] **Wolfgang Schäfer**[c] **and Antoni Szczurek**[c]

[a] *Faculty of Mathematics and Natural Sciences, University of Rzeszów, ul. Pigonia 1, PL-35-310 Rzeszów, Poland*
[b] *Helsinki Institute of Physics, P.O. Box 64 (Gustaf Hällströmin katu 2), FI-00014 University of Helsinki, Helsinki, Finland*
[c] *Institute of Nuclear Physics Polish Academy of Sciences, ul. Radzikowskiego 152, PL-31-342 Kraków, Poland*

E-mail: luszczak@ur.edu.pl, laurent.forthomme@cern.ch, wolfgang.schafer@ifj.edu.pl, antoni.szczurek@ifj.edu.pl

Abstract: We discuss the production of $t\bar{t}$ quark-antiquark pairs in proton-proton collisions via the $\gamma\gamma$ fusion mechanism. We include topologies in which both protons stay intact or one or even both of them undergo dissociation. The calculations are performed within the k_T-factorisation approach, including transverse momenta of intermediate photons. Photon fluxes associated with inelastic (dissociative) processes are calculated based on modern parameterisations of proton structure functions. We find an integrated cross section of about 2.36 fb at $\sqrt{s} = 13$ TeV for all contributions (without requirement of rapidity gap). The cross section for the fully elastic process is the smallest. Inelastic contributions are significantly reduced when a veto on outgoing jets is imposed. We present several differential distributions in rapidity and transverse momenta of single t or $\bar{t}$ quarks/antiquarks as well as distributions in invariant mass of both the $t\bar{t}$ and masses of dissociated systems. A few two-dimensional distributions are presented in addition.

Keywords: Phenomenological Models, QCD Phenomenology

ArXiv ePrint: 1810.12432

Open Access, © The Authors.
Article funded by SCOAP[3].

https://doi.org/10.1007/JHEP02(2019)100

JHEP02(2019)100

Contents

JHEP02(2019)100

1 Introduction

Photon-induced processes in proton-proton or nucleus-nucleus interactions have become very topical recently. The large energy at the LHC, when combined with relatively large luminosity at run II, allows to start the exploration of such processes. Although in the case of proton-proton collisions the relevant cross sections are rather small, some of their salient features may allow their measurement. For instance, photon-fusion events will lead to a rapidity gap observable experimentally between the electromagnetic/electroweak vertex and forward scattered systems.

The production of electron or muon pairs are flag examples. Recently both CMS [1–3] and ATLAS [4] studied such processes. Another example is the production of W^+W^- pairs also studied by both Collaborations [5–7]. These results allow to obtain upper limits on the deviations from Standard Model couplings. On the theoretical side such processes may be calculated using the equivalent photon approximation for purely elastic and partially or fully inelastic processes [8]. The photon flux corresponding to the elastic part is then expressed in terms of electromagnetic form factors of proton (electric and magnetic, or equivalently Dirac and Pauli). Proton dissociative processes need as an input the structure functions F_2 and F_L of a proton, here especially F_2 is well known in a broad kinematic range from a large body of deep-inelastic electron-proton scattering data.

A similar method was used in the $k_{\rm T}$-factorisation approach for dilepton production [9, 10] and recently for W^+W^- production [11]. Actually a similar approach was suggested for lepton pairs long time ago in [12] and realised in the LPAIR code [13].

Different parameterisations of the proton structure functions were used in the literature. The overall errors/uncertainties are therefore associated with insufficient knowledge of structure functions and/or poor functional form of parameterising the data. In [14, 15] it was argued that parameterisations based on proton structure functions have much smaller uncertainties, and generally lead to much smaller cross sections than in the standard DGLAP approach.

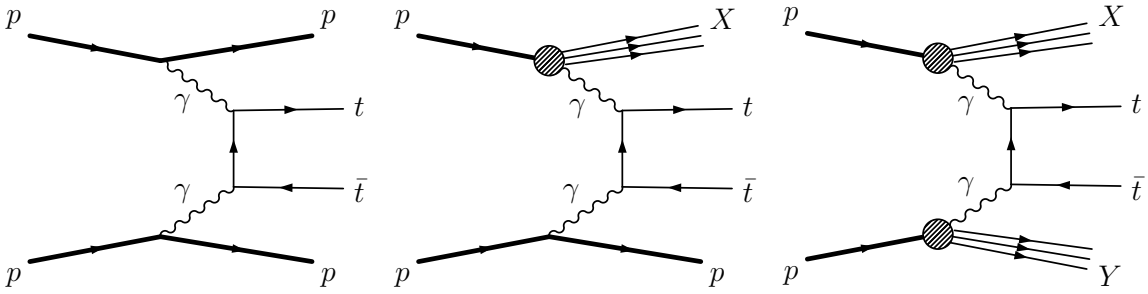

Figure 1. Classes of processes discussed in the present paper. From left to right: elastic-elastic, inelastic-elastic (or equivalently, elastic-inelastic), and inelastic-inelastic contributions.

In the present approach we study a new final state, namely t and $\bar{t}$. Being the heaviest of fundamental Standard Model particles, the top quark is of special interest. The dominant production mechanisms investigated until recently in great detail involve the strong interactions. While the precision studies of electroweak production mechanisms are clearly the task for an e^+e^- collider [16], here we wish to investigate the $\gamma\gamma$ fusion contribution in pp collisions at the LHC.

There has not been much discussion of this final state in the literature in the context of the $\gamma\gamma$ fusion. In ref. [17], the fully exclusive $pp \to ppt\bar{t}$ process was discussed at LHC energies, including possible anomalous $\gamma t\bar{t}$ couplings. A very comprehensive study [18] includes electroweak corrections to inclusive $t\bar{t}$ production. Being a part of these corrections, the $\gamma\gamma$ fusion subprocess is evaluated using collinear photon parton distributions. The $\gamma\gamma$ contribution to inclusive $t\bar{t}$ production is found to be negligible, when realistic photon distributions are used.

In figure 1 we show diagrams of the four different classes of processes included in our present analysis. In the present paper we concentrate on general characteristics and study of differential distribution to select a proper observable for future experimental studies.

We wish to evaluate the cross section separately for each category presented in the figure within the Standard Model. We also aim at calculating several differential distributions of interest.

2 A sketch of the formalism

Our calculations are based on the elastic and the inelastic photon fluxes. The unintegrated photon fluxes can be obtained using the following equation [9, 10]:

$$\gamma^p_{\rm in}(x,\vec{q}_T) = \frac{1}{x}\frac{1}{\pi\vec{q}_T{}^2}\int_{M^2_{\rm thr}} dM_X^2 \mathcal{F}^{\rm in}_{\gamma^*\leftarrow p}(x,\vec{q}_T,M_X^2)\,, \tag{2.1}$$

and we use the functions $\mathcal{F}^{\rm in}_{\gamma^*\leftarrow p}$ from [8, 11]:

$$\mathcal{F}^{\rm in}_{\gamma^*\leftarrow p}(x,\vec{q}_T) = \frac{\alpha_{\rm em}}{\pi}\left\{(1-x)\left(\frac{\vec{q}_T{}^2}{\vec{q}_T{}^2+x(M_X^2-m_p^2)+x^2m_p^2}\right)^2\frac{F_2(x_{\rm Bj},Q^2)}{Q^2+M_X^2-m_p^2}\right.$$
$$\left. + \frac{x^2}{4x_{\rm Bj}^2}\frac{\vec{q}_T{}^2}{\vec{q}_T{}^2+x(M_X^2-m_p^2)+x^2m_p^2}\frac{2x_{\rm Bj}F_1(x_{\rm Bj},Q^2)}{Q^2+M_X^2-m_p^2}\right\}. \tag{2.2}$$

JHEP02(2019)100

The virtuality Q^2 of the photon depends on the photon transverse momentum ($\vec{q}_T{}^2$) and the proton remnant mass (M_X):

$$Q^2 = \frac{\vec{q}_T{}^2 + x(M_X^2 - m_p^2) + x^2 m_p^2}{(1-x)}\,. \tag{2.3}$$

The proton structure functions $F_1(x_{\rm Bj}, Q^2)$ and $F_2(x_{\rm Bj}, Q^2)$ require the argument

$$x_{\rm Bj} = \frac{Q^2}{Q^2 + M_X^2 - m_p^2}. \tag{2.4}$$

In eq. (2.2) we in practise use the pair $F_2(x_{\rm Bj}, Q^2), F_L(x_{\rm Bj}, Q^2)$, where

$$F_L(x_{\rm Bj}, Q^2) = \left(1 + \frac{4x_{\rm Bj}^2 m_p^2}{Q^2}\right) F_2(x_{\rm Bj}, Q^2) - 2x_{\rm Bj} F_1(x_{\rm Bj}, Q^2) \tag{2.5}$$

is the longitudinal structure function of the proton. We obtain the elastic photon fluxes for the proton similarly as for the inelastic piece, and expressed as in ref. [8] as:

$$\mathcal{F}^{\rm el}_{\gamma^*\leftarrow p}(x, \vec{q}_T) = \frac{\alpha_{\rm em}}{\pi}(1-x)\left(\frac{\vec{q}_T{}^2}{\vec{q}_T{}^2 + x^2 m_p^2}\right)^2 \left[\left(1 - \frac{x}{2}\right)^2 \frac{4m_p^2 G_E^2(Q^2) + Q^2 G_M^2(Q^2)}{4m_p^2 + Q^2} + \frac{x^2}{4} G_M^2(Q^2)\right]. \tag{2.6}$$

The photon virtuality Q^2 for the elastic flux can be obtained from eq. (2.3) for $M_X = m_p$. Then in analogy to eq. (2.1)

$$\gamma^p_{\rm el}(x, \vec{q}_T) = \frac{1}{x}\frac{1}{\pi \vec{q}_T{}^2}\, \mathcal{F}^{\rm el}_{\gamma^*\leftarrow p}(x, \vec{q}_T). \tag{2.7}$$

The full photon flux is then

$$\frac{d\gamma(x, \vec{q}_T, M_X)}{dM_X} = \delta(M_X - m_p)\gamma^p_{\rm el}(x, \vec{q}_T) + \frac{d\gamma^p_{\rm in}(x, \vec{q}_T, M_X)}{dM_X}\,. \tag{2.8}$$

Here we put in evidence the contributions of "elastic" processes with an intact proton in the final state as well as the "inelastic" component for hadronic final states $X \neq p$. The photon fluxes enter the $p + p \to X + (\gamma^*\gamma^* \to t\bar{t}) + Y$ production cross section as:

$$\frac{d\sigma(pp \to X(\gamma^*\gamma^* \to t\bar{t})Y)}{dy_+ dy_- d^2\vec{p}_{T1} {\rm d}^2\vec{p}_{T2} dM_X dM_Y} = \int d^2\vec{q}_{T1} d^2\vec{q}_{T2} \frac{x_1 d\gamma(x_1, \vec{q}_{T1}, M_X)}{dM_X} \frac{x_2 d\gamma(x_2, \vec{q}_{T2}, M_Y)}{dM_Y} \times \frac{1}{16\pi^2 (x_1 x_2 s)^2} |M(\gamma^*\gamma^* \to t\bar{t}; \vec{q}_{T1}, \vec{q}_{T2})|^2\, \delta^{(2)}(\vec{p}_{T1} + \vec{p}_{T2} - \vec{q}_{T1} - \vec{q}_{T2}). \tag{2.9}$$

In this formalism $y_\pm$ are the rapidities and $\vec{p}_{T1,2}$ the transverse momenta of the t and $\bar{t}$ quark respectively. The off-shell matrix element squared for the $\gamma^*\gamma^* \to t\bar{t}$ process is the same as the one for dilepton production found in [9], up to a factor $e_f^4 N_c$, with $e_f = +2/3$ the quark electric charge, and $N_c = 3$. In results shown below we use the top quark mass $m_t = 173\,{\rm GeV}$.

JHEP02(2019)100

Contribution	No cuts	$y_{\rm jet}$ cut
elastic-elastic	0.292	0.292
elastic-inelastic	0.544	0.439
inelastic-elastic		
inelastic-inelastic	0.983	0.622
all contributions	2.36	1.79

Table 1. Cross section in fb at $\sqrt{s} = 13\,\text{TeV}$ for different components (left column) and the same when the extra condition on the outgoing jet $|y_{\rm jet}| > 2.5$ is imposed.

More details on the proton structure functions may be found in [11], where we describe several parameterisations used for F_2, F_L. Here we only mention that in the region of $Q^2 > 9\,\text{GeV}^2$, which is the most important one for the process at hand, we use a perturbative QCD NNLO calculation of [19].

3 Results

In table 1 we show integrated cross sections for each of the categories of $\gamma\gamma$ processes shown in figure 1. We observe the following hierarchy as far as the integrated cross section is considered:

$$\sigma_{t\bar{t}}^{\rm el-el} < \sigma_{t\bar{t}}^{\rm in-el} = \sigma_{t\bar{t}}^{\rm el-in} < \sigma_{t\bar{t}}^{\rm in-in}. \tag{3.1}$$

The summed inclusive cross section at $\sqrt{s} = 13\,\text{TeV}$ is 2.36 fb. This is a rather small number in comparison with other inclusive production mechanisms. A possible extraction of $\gamma\gamma$ events therefore requires, e.g. experimental cuts on rapidity gaps. So far we have ignored the gap survival factor due to remnant fragmentation and/or soft processes. However, such effects may reverse the order of eq. (3.1). This behaviour was obtained previously for production of W^+W^- pairs via $\gamma - \gamma$ fusion in [20].

In the right panel of table 1 we show results when a rapidity gap[1] in the central region, for $-2.5 < y < 2.5$ is required in addition. In principle, imposing this condition requires modelling of the full final state, as we did for the case of W^+W^- production in [20]. As in each event we have the full four-momentum of the virtual photon(s), as well as the invariant masses of the proton remnants, the four-momenta of the recoiling jet(s) can be reconstructed (see [20]). To a good accuracy the rapidity gap condition is equivalent to require that the recoiling jets fulfill $|y_{\rm jet}| > 2.5$. This has been checked in [20] by including explicitly remnant fragmentation.

In figure 2 we show the rapidity distributions of t quarks or $\bar{t}$ antiquarks (these are identical) for different categories of the final state.[2] Quite similar distributions are obtained for the different categories of processes. There is only a small asymmetry with respect to $y = 0$ for elastic-inelastic or inelastic-elastic contributions. By construction, the sum of both

[1] That means no additional particle production except the t or $\bar{t}$.

[2] LUX-like means our parametrization of the structure function done in a way proposed in [11].

JHEP02(2019)100

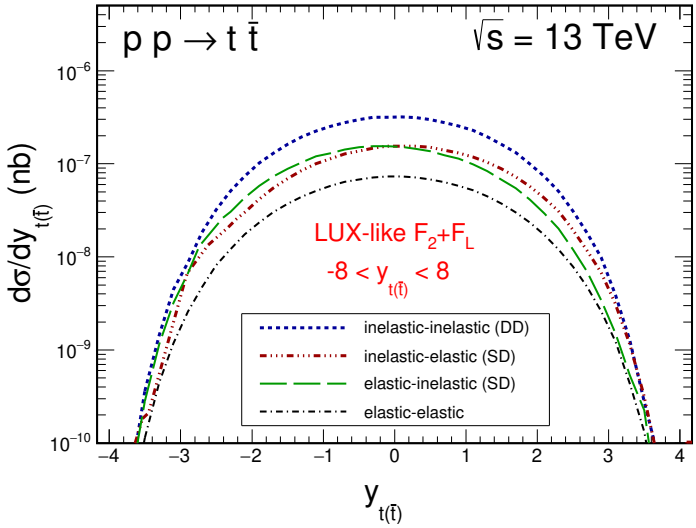

Figure 2. Rapidity distribution of t or $\bar{t}$ for different components defined in the figure.

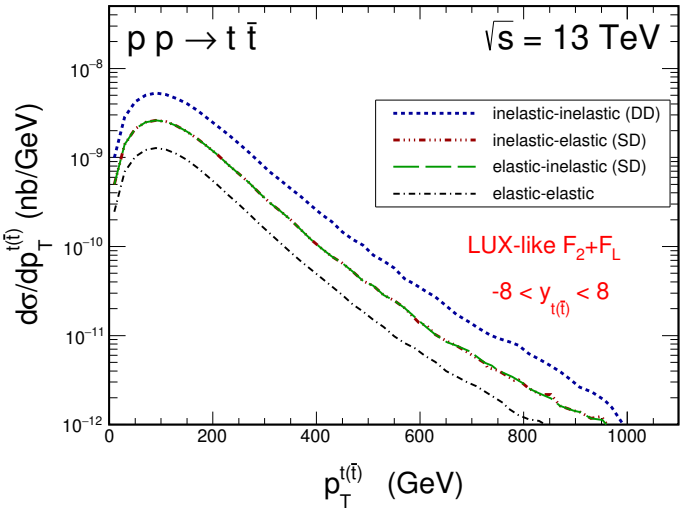

Figure 3. Transverse momentum distribution of t or $\bar{t}$ for different components defined in the figure.

the contributions is symmetric with respect to $y = 0$. The cross section is concentrated at intermediate rapidities so in principle should be measurable by the ATLAS/CMS central detectors. However, a precise estimation would require imposing cuts on the decay products of t and $\bar{t}$ (for instance, into a b jet and a charged lepton). This goes beyond scope and aim of the present work.

In figure 3 we show the distribution in transverse momentum of t or $\bar{t}$ (identical). Here again the different categories give distributions of similar shape.

The same is true for the distribution in $t\bar{t}$ invariant mass (see the left panel of figure 4). The distributions are almost identical and differ only by normalisation. For completeness in the right panel of figure 4 we show similar results when conditions on outgoing light

JHEP02(2019)100

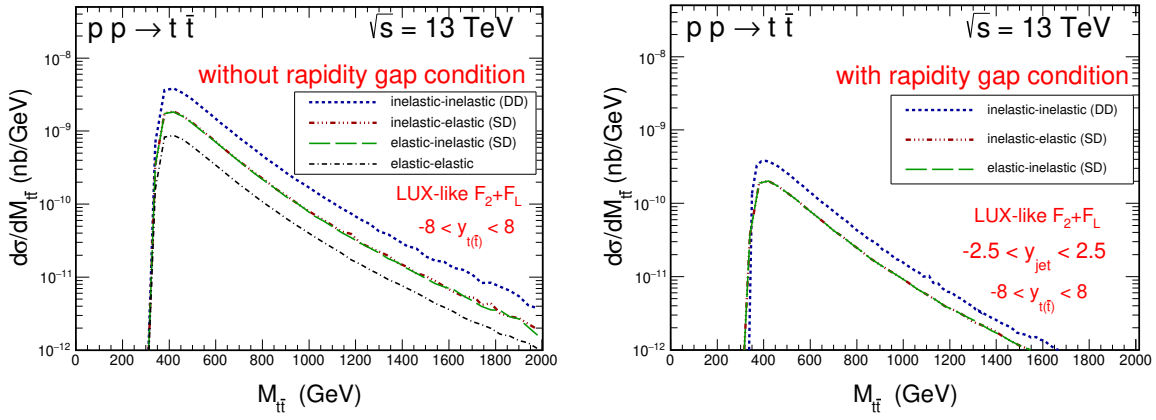

Figure 4. $t\bar{t}$ invariant mass distribution for different components defined in the figure. The left panel is without imposing the condition on the struck quark/antiquark and the right panel includes the condition.

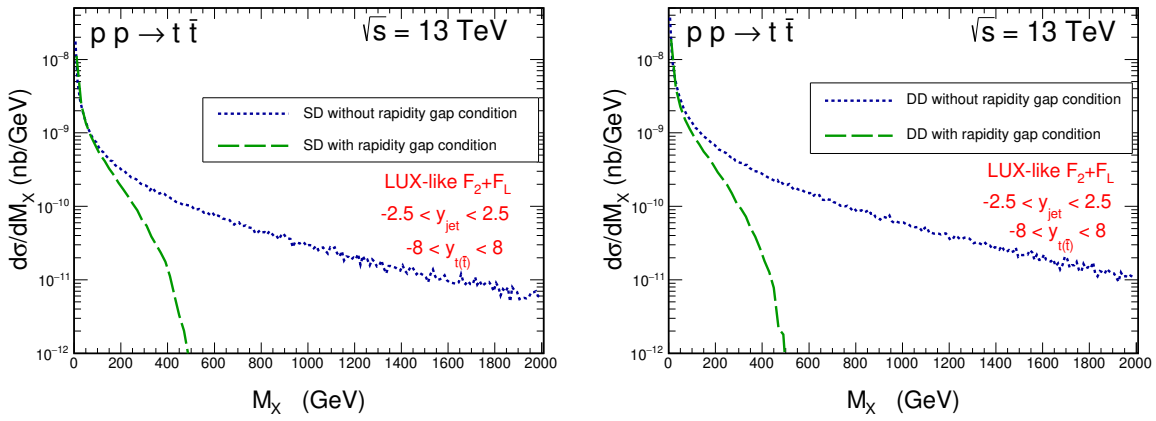

Figure 5. Distribution in the mass of the dissociated system for single dissociation (left) and double dissociation (right). We show result without and with the rapidity gap condition.

quark/antiquark jets are imposed. The extra condition leads to a lowering of the cross section with only very small modification of the shape in $M_{t\bar{t}}$.

In addition in figure 5 we show distributions in outgoing proton remnant masses M_X and/or M_Y. Similar shapes are observed for single-dissociative and double-dissociative processes. Population of large M_X or M_Y masses is associated with the emissions of jets visible in central detectors (i.e. with $-2.5 < y_{\rm jet} < 2.5$). We show the distribution in the remnant mass M_X separately for the single dissociation (left) and double dissociation (right). As can be seen, the rapidity gap requirement introduces a rather sharp cut-off in the large-mass tail of the M_X-distribution.

In figure 6 we show distribution in photon virtuality. One may notice the photon emission through proton dissociation is much broader than that for elastic production. A large contribution to the cross section is hence shown to arise from the region of highly virtual photons, $Q^2 > 1000\,{\rm GeV}^2$.

JHEP02(2019)100

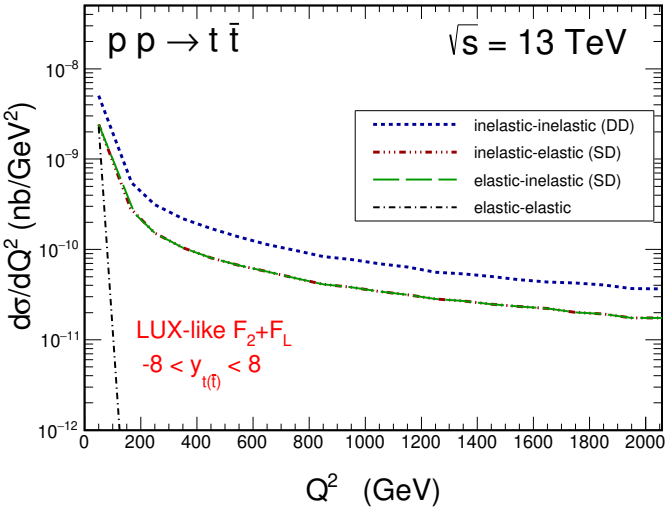

Figure 6. Photon virtuality distribution for different components defined in the figure.

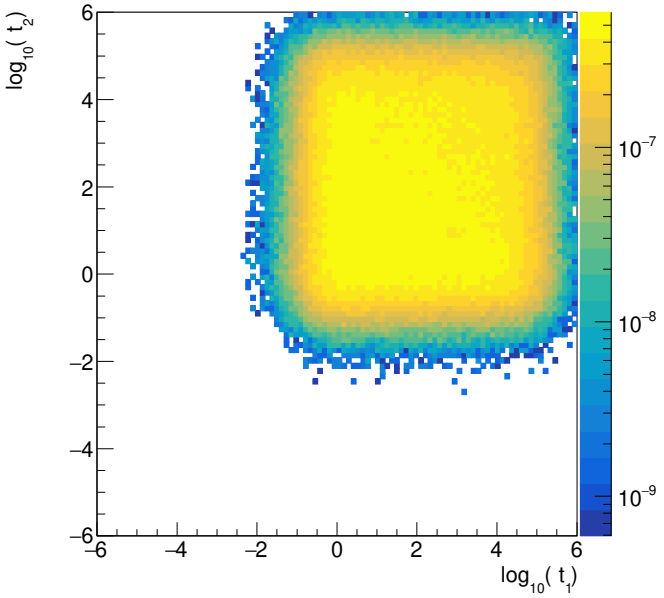

Figure 7. The two-dimensional $\frac{d^2\sigma}{d\log_{10}(-t_1)d\log_{10}(-t_2)}$ distribution as a function of $\log_{10}(-t_1)$, $\log_{10}(-t_2)$ in nb for the inelastic-inelastic contribution. Here $Q_i^2 = -t_i \cdot 1\,\mathrm{GeV}^2$.

Finally we wish to show some two-dimensional distributions in $Q_1^2 \times Q_2^2$ (figure 7) and $M_X \times M_Y$ (figure 8) for inelastic-inelastic case. In figure 7 we see regions when both photon virtualities are large.

In figure 9 we show distributions in M_X for a fixed M_Y (left panel) and in M_Y for a fixed M_X (right panel). The distributions are arbitrarily normalized to the same integral. All the distributions coincide. This means that the two-dimensional distribution can be factorized:

$$\frac{d\sigma(M_X, M_Y)}{dM_X dM_Y} = Cf(M_X)f(M_Y). \tag{3.2}$$

Similar discussion concerns also our recent study of W^+W^- production [20].

JHEP02(2019)100

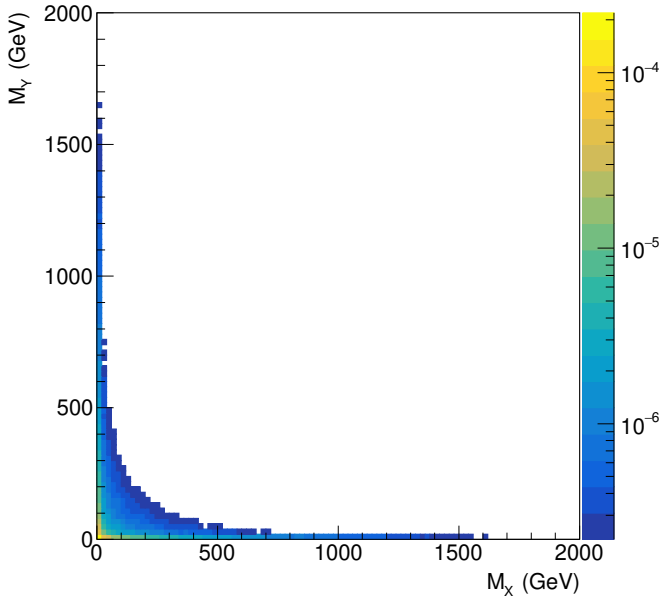

Figure 8. The two-dimensional $\frac{d^2\sigma}{dM_X\,dM_Y}$ distribution as a function of $M_X \times M_Y$ in nb/GeV^2 for the inelastic-inelastic contribution.

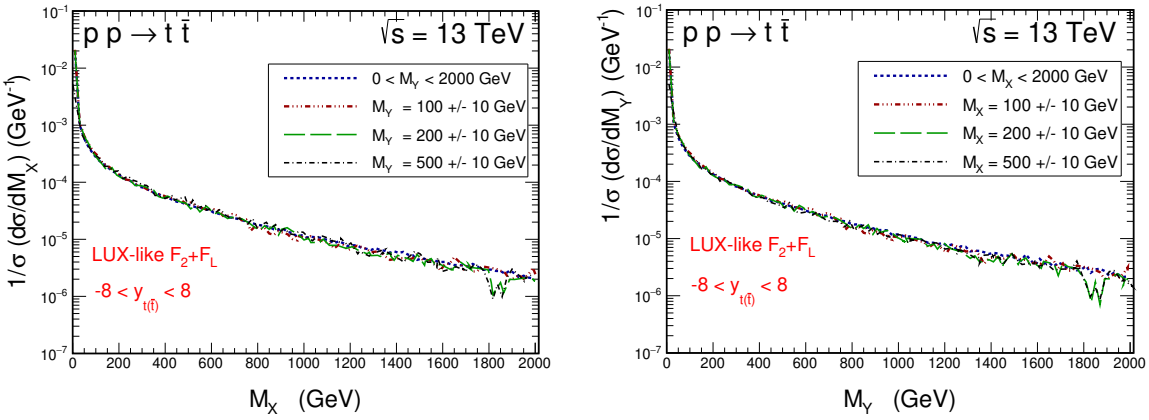

Figure 9. Distribution in M_X for different widnows of M_Y (left) and as a function of M_Y for different windows of M_X (right).

Finally in figure 10 we show distribution in $p_{\mathrm{T,sum}} = |\vec{p}_{\mathrm{T}1} + \vec{p}_{\mathrm{T}2}|$. The distribution for the elastic-elastic component is much narrower than similar distributions for the other components. We note that for collinear photon distributions we would obtain in the leading-order approximation a delta-function in $p_{\mathrm{T,sum}}$. Generation of finite $p_{\mathrm{T,sum}}$ would require the evaluation of higher-order contributions.

4 The gap survival factor

It is useful to present the effect of the rapidity-gap veto in the form of a gap-survival factor. Here we follow the procedure of [20] where the analogous physics for the $\gamma\gamma \to W^+W^-$ production was discussed.

JHEP02(2019)100

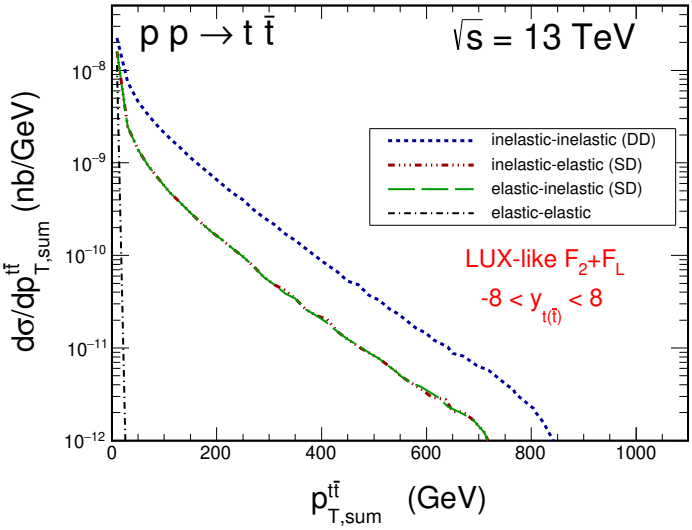

Figure 10. Distribution in transverse momentum of the t and $\bar{t}$ pairs for elastic - elastic, inelastic-elastic (elastic-inelastic) and inelastic-inelastic contributions for LUX-like structure function.

As the rapidity gap is potentially destroyed by a parton (jet or mini-jet), which is struck by the virtual photon out of the proton, we define a gap survival factor as simply the fraction of events with no jet in the veto region $-\eta_{\rm cut} < \eta_{\rm jet} < \eta_{\rm cut}$:

$$S_R(\eta_{\rm cut}) = 1 - \frac{1}{\sigma}\int_{-\eta_{\rm cut}}^{\eta_{\rm cut}} \frac{{\rm d}\sigma}{{\rm d}\eta_{\rm jet}}{\rm d}\eta_{\rm jet}, \tag{4.1}$$

where ${\rm d}\sigma/{\rm d}\eta_{\rm jet}$ is the cross section for $t\bar{t}$ production (integrated over all kinematical variables) differential in the rapidity of the extra jet (de facto parton) and σ is the associated integrated cross section. In principle, the gap survival factor could be also defined differentially in the t or $\bar{t}$ kinematic variables, but here we restrict ourselves to the fully integrated case. This plot summarizes how much of the cross section would be lost by imposing the rapidity gap condition.

Here, in figure 12 we show our results for $pp \to \gamma\gamma \to t\bar{t}$ processes. The gap survival factor is $S_R^{DD} < S_R^{SD}$. We have checked that the factorisation $S_R^{DD} = (S_R^{SD})^2$ holds to very good accuracy. One may note the magnitude of such gap survival factors can reverse the ordering in (3.1) for large η_{cut}.

The $\gamma\gamma$ contribution to inclusive $t\bar{t}$ production is small. How could one therefore "measure" or extract the $\gamma\gamma$ contribution? Requiring a rapidity gap (rapidity region free of additional particles) is a pragmatic solution. In the present analysis for illustration we have taken the rapidity interval $-2.5 < y < 2.5$ which should be free of particles (this does not include t or $\bar{t}$ or their decay products which could fall into this interval).

In principle, besides the remnant fragmentation there are also other mechanisms which can fill up a rapidity gap which should be included. In the present analysis we include only (mini)jet emission(s) from remnant(s) (as in ref. [20]). Soft interactions between spectator partons could also lead to additional production which destroys the rapidity gap condition. However, as discussed in [20], the relevant formalism for proton electromagnetic dissociative

JHEP02(2019)100

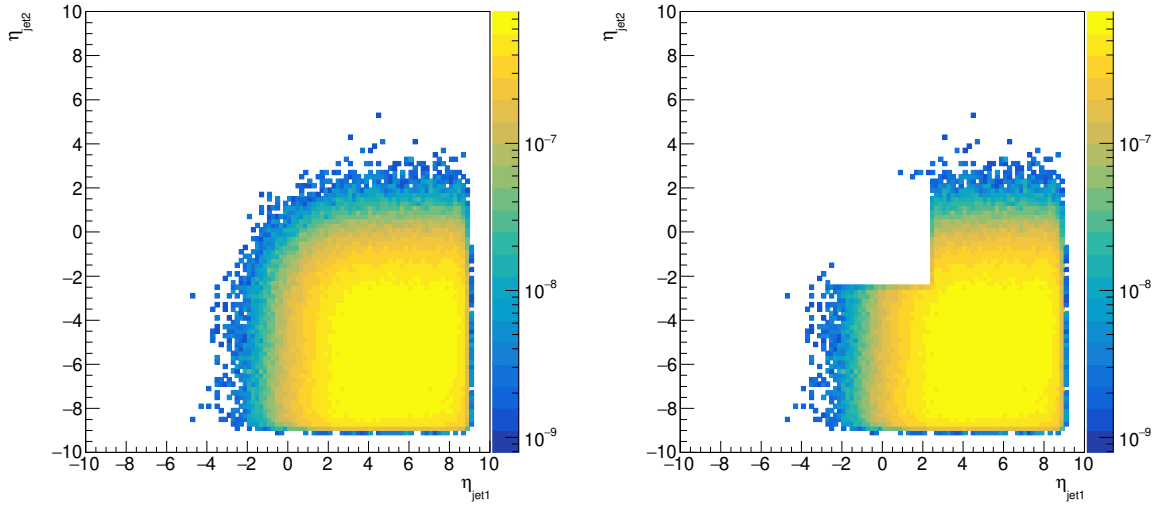

Figure 11. The two-dimensional $\frac{d^2\sigma}{d\eta_{\rm jet1}d\eta_{\rm jet2}}$ distribution as a function of $\eta_{\rm jet1}, \eta_{\rm jet2}$ in nb. The left panel shows distribution without cuts and the right panel with cuts on $\eta_{\rm jet1}$ and $\eta_{\rm jet2}$.

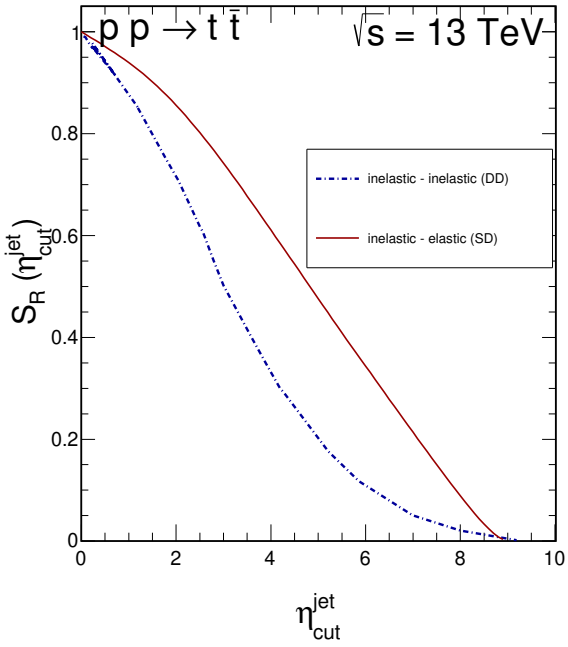

Figure 12. Gap survival factor for single and double dissociation as a function of the size of the pseudorapidity veto applied on the recoiling jet emitted from proton remnants.

processes with large excited masses was not yet worked out. These contributions should be studied in future also as a function of the size of the rapidity gap window in order to make fully quantitative comparison of theoretical calculations with future experimental data. However, this clearly goes beyond the scope of the present paper.

JHEP02(2019)100

5 Conclusions

In the present paper we have presented cross sections for production of $t\bar{t}$ pairs via $\gamma^*\gamma^*$ fusion. Such processes can be separated out by imposing rapidity gaps in the central detector. Our calculations include transverse momenta of the intermediate photons. The flux of photons produced with proton dissociation has been expressed in terms of proton structure functions. For our study we have used a hybrid parameterisation of proton structure functions, using similar input as the recent LUXqed parameterisation [15].

The cross section summed over the different categories of processes is about 2.36 fb (full phase space), i.e. rather small compared to the standard inclusive $t\bar{t}$ cross section (of the order of nb). We have shown that the ordering (3.1) holds for the whole phase space without extra experimental conditions on the top quarks decay products reconstruction efficiencies and central system gap survival factor. As discussed recently in ref. [20] for the W^+W^- final state, the remnant fragmentation leads to a taming of the cross section when the rapidity gap requirement is imposed. Also here such a condition reverses the hierarchy observed for the case when such condition is taken into account.

One may argue that a diffractive QCD contribution leads to the same rapidity-gap topology as $\gamma\gamma$-fusion. We have checked, that using the formalism of [21, 22], the cross section for a QCD diffractive contribution to the $t\bar{t}$ production is about 2-3 orders of magnitude smaller than the one corresponding to the photon-photon fusion and does need to be included in the final estimate. This is very different than for "exclusive" $c\bar{c}$ [21] or $b\bar{b}$ [22] production. We have presented several differential distributions in rapidity and transverse momentum of the t or $\bar{t}$ as well as invariant mass of the $t\bar{t}$ system or in the mass of the dissociated proton system. We have shown also some correlation distributions, some of them two-dimensional ones.

Our results imply that for the production of such heavy objects as t quark and $\bar{t}$ antiquark the virtuality of the photons attached to the dissociative system are very large ($Q^2 < 10^4\,\mathrm{GeV}^2$). A similar effect was discussed in detail already for the W^+W^- system [11].

We have presented the best estimate of the cross section(s) and differential distributions for the inclusive case (no requirement on rapidity gap) as well as including extra condition on the jet rapidity. Applying a veto on charged particles or outgoing jet in a certain rapidity region (as done here) lowers the cross section significantly. As the gluon-gluon fusion cross section is so large, rapidity gap fluctuations in the hadronisation can be a serious background. The gap must then be chosen to minimise the unwanted contributions from gluon-gluon and quark-antiquark subprocesses not loosing too much of the signal ($\gamma\gamma \to t\bar{t}$ contribution). Evaluating such an effect will be necessary to demonstrate whether the Standard Model $\gamma\gamma \to t\bar{t}$ contribution can be "observed" at the LHC.

Acknowledgments

This study was partially supported by the Polish National Science Centre grants DEC-2014/15/B/ST2/02528 and by the Center for Innovation and Transfer of Natural Sciences and Engineering Knowledge in Rzeszów.

JHEP02(2019)100

Open Access. This article is distributed under the terms of the Creative Commons Attribution License (CC-BY 4.0), which permits any use, distribution and reproduction in any medium, provided the original author(s) and source are credited.

References

[1] CMS collaboration, *Exclusive photon-photon production of muon pairs in proton-proton collisions at* $\sqrt{s} = 7$ *TeV*, *JHEP* **01** (2012) 052 [arXiv:1111.5536] [INSPIRE].

[2] CMS collaboration, *Search for exclusive or semi-exclusive photon pair production and observation of exclusive and semi-exclusive electron pair production in pp collisions at* $\sqrt{s} = 7$ *TeV*, *JHEP* **11** (2012) 080 [arXiv:1209.1666] [INSPIRE].

[3] CMS and TOTEM collaborations, *Observation of proton-tagged, central (semi)exclusive production of high-mass lepton pairs in pp collisions at 13 TeV with the CMS-TOTEM precision proton spectrometer*, *JHEP* **07** (2018) 153 [arXiv:1803.04496] [INSPIRE].

[4] ATLAS collaboration, *Measurement of exclusive* $\gamma\gamma \to \ell^+\ell^-$ *production in proton-proton collisions at* $\sqrt{s} = 7$ *TeV with the ATLAS detector*, *Phys. Lett.* **B 749** (2015) 242 [arXiv:1506.07098] [INSPIRE].

[5] CMS collaboration, *Study of exclusive two-photon production of* W^+W^- *in pp collisions at* $\sqrt{s} = 7$ *TeV and constraints on anomalous quartic gauge couplings*, *JHEP* **07** (2013) 116 [arXiv:1305.5596] [INSPIRE].

[6] CMS collaboration, *Evidence for exclusive* $\gamma\gamma \to W^+W^-$ *production and constraints on anomalous quartic gauge couplings in pp collisions at* $\sqrt{s} = 7$ *and* 8 *TeV*, *JHEP* **08** (2016) 119 [arXiv:1604.04464] [INSPIRE].

[7] ATLAS collaboration, *Measurement of exclusive* $\gamma\gamma \to W^+W^-$ *production and search for exclusive Higgs boson production in pp collisions at* $\sqrt{s} = 8$ *TeV using the ATLAS detector*, *Phys. Rev.* **D 94** (2016) 032011 [arXiv:1607.03745] [INSPIRE].

[8] V.M. Budnev, I.F. Ginzburg, G.V. Meledin and V.G. Serbo, *The Two photon particle production mechanism. Physical problems. Applications. Equivalent photon approximation*, *Phys. Rept.* **15** (1975) 181 [INSPIRE].

[9] G.G. da Silveira, L. Forthomme, K. Piotrzkowski, W. Schäfer and A. Szczurek, *Central* $\mu^+\mu^-$ *production via photon-photon fusion in proton-proton collisions with proton dissociation*, *JHEP* **02** (2015) 159 [arXiv:1409.1541] [INSPIRE].

[10] M. Łuszczak, W. Schäfer and A. Szczurek, *Two-photon dilepton production in proton-proton collisions: two alternative approaches*, *Phys. Rev.* **D 93** (2016) 074018 [arXiv:1510.00294] [INSPIRE].

[11] M. Łuszczak, W. Schäfer and A. Szczurek, *Production of* W^+W^- *pairs via* $\gamma^*\gamma^* \to W^+W^-$ *subprocess with photon transverse momenta*, *JHEP* **05** (2018) 064 [arXiv:1802.03244] [INSPIRE].

[12] J.A.M. Vermaseren, *Two Photon Processes at Very High-Energies*, *Nucl. Phys.* **B 229** (1983) 347 [INSPIRE].

[13] S.P. Baranov, O. Duenger, H. Shooshtari and J.A.M. Vermaseren, *LPAIR: A generator for lepton pair production*, in *Workshop on Physics at HERA*, Hamburg, Germany, October 29–30, 1991, pp. 1478–1482 (1991) [INSPIRE].

JHEP02(2019)100

[14] A. Manohar, P. Nason, G.P. Salam and G. Zanderighi, *How bright is the proton? A precise determination of the photon parton distribution function*, *Phys. Rev. Lett.* **117** (2016) 242002 [arXiv:1607.04266] [INSPIRE].

[15] A.V. Manohar, P. Nason, G.P. Salam and G. Zanderighi, *The Photon Content of the Proton*, *JHEP* **12** (2017) 046 [arXiv:1708.01256] [INSPIRE].

[16] CLICDP collaboration, *Top-Quark Physics at the CLIC Electron-Positron Linear Collider*, arXiv:1807.02441 [INSPIRE].

[17] S. Fayazbakhsh, S.T. Monfared and M. Mohammadi Najafabadi, *Top Quark Anomalous Electromagnetic Couplings in Photon-Photon Scattering at the LHC*, *Phys. Rev.* **D 92** (2015) 014006 [arXiv:1504.06695] [INSPIRE].

[18] M. Czakon, D. Heymes, A. Mitov, D. Pagani, I. Tsinikos and M. Zaro, *Top-pair production at the LHC through NNLO QCD and NLO EW*, *JHEP* **10** (2017) 186 [arXiv:1705.04105] [INSPIRE].

[19] A.D. Martin, W.J. Stirling, R.S. Thorne and G. Watt, *Parton distributions for the LHC*, *Eur. Phys. J.* **C 63** (2009) 189 [arXiv:0901.0002] [INSPIRE].

[20] L. Forthomme, M. Łuszczak, W. Schäfer and A. Szczurek, *Rapidity gap survival factors caused by remnant fragmentation for W^+W^- pair production via $\gamma^*\gamma^* \to W^+W^-$ subprocess with photon transverse momenta*, *Phys. Lett.* **B 789** (2019) 300 [arXiv:1805.07124] [INSPIRE].

[21] A. Szczurek, *Production of digluon and quark-antiquark dijets in central exclusive processes*, in *Proceedings, 14th Workshop on Elastic and Diffractive Scattering (EDS Blois Workshop)on Frontiers of QCD: From Puzzles to Discoveries*, Qui Nhon, Vietnam, December 15–21, 2011 (2012) [arXiv:1204.0340] [INSPIRE].

[22] R. Maciula, R. Pasechnik and A. Szczurek, *Exclusive $b\bar{b}$ pair production and irreducible background to the exclusive Higgs boson production*, *Phys. Rev.* **D 82** (2010) 114011 [arXiv:1006.3007] [INSPIRE].

JHEP02(2019)100